Surface modification of polyethylene with multi-end functional polyethylene additives

AUTHOR NAMES

*Sarah J. Hardman[1], Lian R. Hutchings[1], Nigel Clarke[1,2], Solomon M. Kimani[1], Emily F. Smith[3], John R.P. Webster[4] and Richard L. Thompson[1]**

AUTHOR ADDRESS

1 Durham Centre for Soft Matter, Department of Chemistry, Science Site, Durham, DH1 3LE, UK

2 Present address: School of Physics and Astronomy, Hicks Building, University of Sheffield, Sheffield, UK

3 XPS Laboratory, School of Chemistry, University of Nottingham, University Park, Nottingham, NG7 2RD, UK

4 STFC ISIS Facility, Rutherford Appleton Laboratories, Chilton, Didcot, Oxfordshire, OX11 0QX, UK

AUTHOR EMAIL ADDRESS r.l.thompson@durham.ac.uk

RECEIVED DATE (to be automatically inserted after your manuscript is accepted if required according to the journal that you are submitting your paper to)

TITLE RUNNING HEAD Surface modifying end-functional polyethylene additives.

CORRESPONDING AUTHOR FOOTNOTE

* r.l.thompson@durham.ac.uk

tel +44 191 3342139

fax +44 191 334 4737

ABSTRACT

We have prepared and characterized a series of multi-fluorocarbon end-functional polyethylene additives, which when blended with polyethylene matrices increase surface hydrophobicity and lipophobicity. Water contact angles of >112° were observed on spin-cast blended film surfaces containing less than 1% fluorocarbon in the bulk. Crystallinity in these films gives rise to surface roughness that is an order of magnitude greater than is typical for amorphous spin-cast films, but is too little to give rise to superhydrophobicity. X-ray photoelectron spectroscopy (XPS) confirms the enrichment of the multi-fluorocarbon additives at the air surface by up to 80 times the bulk concentration. Ion beam analysis was used to quantify the surface excess of the additives as a function of composition, functionality and molecular weight of either blend component. In some cases, an excess of the additives was also found at the substrate interface, indicating phase separation into self-stratified layers. The combination of neutron reflectometry and ion beam analysis allowed the surface excess to be quantified above and below the melting point of the blended films. In these films, where the melting temperatures of the additive and matrix components are relatively similar (within 15 °C) the surface excess is almost independent of whether the blended film is semicrystalline or molten, suggesting that the additive undergoes co-crystallization with the matrix when the blended films are allowed to cool below the melting point.

KEYWORDS (Word Style "BG_Keywords").

Polyethylene, surface modification, fluorocarbon, segregation, hydrophobic, semicrystalline

BRIEFS (WORD Style "BH_Briefs").

Polyethylenes having 2, 3 or 4 C_8F_{17} fluorocarbon functional groups per chain-end increase hydrophobicity and lipophobicity of blended film surfaces above and below the melting transition.

MANUSCRIPT TEXT

Introduction

There is a longstanding interest in bringing new surface properties to polymers, and particularly their films, whilst maintaining favourable bulk properties such as transparency, mechanical strength and dimensional stability. Strategies to achieve surface modification can be broadly subdivided into post-production modification techniques, such as corona discharge,[1] plasma treatment,[2] sputtering[3] and coating,[4] or by masterbatch methods in which additives are included in the polymer prior to processing and designed to migrate to the surface of the product spontaneously.[5]

In recent years we and others have shown that remarkable increases in polymer hydrophobicity can be achieved with polymers having a small amount of fluorine concentrated at one end of the polymer chain.[6-9] When added to homopolymers, multi end-fluorinated chain additives spontaneously migrate to the surface of spin-cast films or electrospun fibers[10] causing a marked increase in both hydrophobicity and lipophobicity, approaching PTFE-like surface properties even when the bulk loading of fluorocarbon is of the order of 1% or less. An attractive feature of this methodology is that the surface modification is achieved without the need for secondary processing steps, making it amenable to batch processes. They also have the potential to migrate to and modify the properties of buried interfaces, which are not accessible to external post-production treatments. Furthermore, the polymeric additives

have less impact on the bulk properties of the polymer matrix than small molecule additives, and may act as a reservoir of spare functionality from which damaged surfaces may be regenerated.[11]

Until now, we have focused on model amorphous systems, which, when compared to semi crystalline polymers, are much more amenable to characterization by techniques such as neutron reflectometry which require very smooth homogeneous surfaces. In fact, studies of end functional polymers in blends with crystalline materials are scarce,[12] despite their ubiquitous importance to many technological areas of application. In many cases, film forming polymers for which there is the greatest demand, and potential arising from surface modification are chemically quite inert and usually semi crystalline; polyethylene (PE), polypropylene (PP) and polyethylene terephthalate (PET) being among the most common of them. Whilst our earlier studies on multi-end functional amorphous materials show very encouraging results in terms of efficient and effective surface modification, the extent to which this methodology can be applied to semi crystalline polymers has not yet been addressed.

Here we present a first comprehensive study of the surface properties of multi-fluorocarbon end functional polyethylenes in thin polyethylene films. In an earlier study by Hirt et al,[12] the potential for modification of linear low density polyethylene (LLDPE) surfaces with C_8F_{17} functionalized linear or branched polymers was identified. However, the additives used in this study were of relatively low molecular weight and did not have the benefit of multiple fluorocarbon groups focused on single chain ends, which we have found to be so effective for surface modification in our earlier work. We address systems in which the molecular weight of the functionalized additive significantly exceeds the entanglement molecular weight in the melt and the functionality is exclusively located at one chain end of the polymer. Such materials combine the optimal topology to modify surfaces most efficiently[13] with a pendant polymer chain of sufficient molecular weight to be anchored into the surface.[14] An additional benefit of this approach is that the bulk properties of the additive such as the melting point are sufficiently similar to those of the matrix to which it is added that processing both components from a single masterbatch becomes a realistic possibility.

The ability of materials that are the subject of this work to crystallize gives rise to the interesting possibility that crystallization could enhance the surface segregation process. This effect has previously been exploited to direct surface segregation of active components for conducting polymer devices.[15] The purpose of this study is therefore to investigate for the first time the application of multi-end functional polymer additives in a matrix of semi crystalline (commodity) polymer (PE), and to quantify the behavior of these materials as a function of their functionality, molecular weight and thermal history.

Experimental Section

Synthesis

Samples of polyethylene additive were prepared by the saturation of end-functional polybutadiene with either deuterium or hydrogen gas.[16] The synthesis of the polybutadiene additives will be described in greater detail elsewhere[17] and the saturation of polybutadiene to make polyethylene-like materials is well reported.[18-20] Briefly, 1,3-butadiene was polymerized by living anionic polymerization using sec-butyllithium as an initiator and hexane as the solvent. The use of a non-polar solvent ensures predominantly 1,4 enchainment of the polybutadiene, and in our case this was consistently 92% ±1% 1,4 enchainment, with the remainder being 1,2 enchainment. The chain-end functionality was introduced via a controlled end capping/termination reactions and prior to end-capping, a sample of polymer was collected and terminated to allow analysis of the molecular weight of the polybutadiene by gel permeation chromatography.

The living polybutadiene chains were capped with diphenylethylene before termination with a multi-C_8F_{17}-fluorocarbon functionalized aryl ether bromide group. The fluorocarbon end-capped polybutadiene additives were saturated with hydrogen or deuterium as required at 500 psi in the presence of a Pd catalyst. The reaction mechanism is summarized in Scheme 1, supporting information.

For convenience, we adopt here a similar notation to our earlier work on amorphous multi end-functionalized polymers; "*x*CF**P***y*", where x is the number functional groups, CF indicates that the

functional groups are C_8F_{17} fluorocarbon groups, **P** is the polymer species, with a molecular weight of approximately *y* kg/mol. It therefore follows that 3CFdPE5 has three C_8F_{17} fluorocarbon groups per deuterated polyethylene (dPE) chain end and the polymer has a molecular weight of approximately 5 kg/mol. Similarly PE100 denotes a non-deuterated unfunctionalised polyethylene chain of approximately 100 kg/mol, which is typical of the matrix materials into which the multi-end functional polyethylene additives are blended.

Thin film preparation

Polyethylene blend films were prepared on silicon substrates by co-dissolution of the functional additives and matrix homopolymers in the desired proportions in warm toluene, such that the total dissolved polymer was approximately 1% (w/w). Thin (~100 nm) blend films were spin-cast using a photoresist spinner operating at ~2000 rpm. In order to prevent precipitation from solution prior to spin-casting and solvent evaporation, it was necessary to pre-heat the silicon substrate on the photoresist spinner for a few seconds before depositing the warmed toluene solution onto the surface. For neutron reflectometry (NR), 5 mm thick, 55 mm diameter silicon substrates were used. Nuclear reaction analysis (NRA), contact angle (CA) analysis, scanning probe microscopy (SPM) and X-ray photoelectron spectroscopy (XPS) experiments were generally carried out on similar films cast onto thinner (~0.7 mm thick) silicon wafers, which were broken into appropriately sized fragments for each experiment. In order to maximize consistency between experiments, several NRA experiments were repeated on thicker substrates which had previously been used in NR experiments. Samples were annealed above their melting point (110 °C) for 1 hour to melt the crystal structure initially formed during spin-casting from solution. These samples were then cooled to below the crystallization temperature (~95 °C) by removal from the oven and allowing them to cool on a bench at room temperature. In some experiments different cooling rates from the molten state were imposed to explore the influence of this parameter on surface structure and composition.

Contact Angle Analysis

Static contact angle analysis was carried out using a manual Rame Hart contact angle goniometer. At least six measurements were carried out on each sample and the error bars given are the standard deviations of these measurements. High purity deionised water was used as the contact fluid. Contact angles of dodecane and glycerol were also carried out on selected specimens with the aim of establishing the lipophobicity and surface energy of the blended films.

X-ray Photoelectron Spectroscopy

XPS experiments were carried out at the University of Nottingham, School of Chemistry. Samples were analyzed using a Kratos AXIS ULTRA DLD X-ray Photoelectron spectroscopy instrument with a monochromated Al K_α X-ray source (1486.6 eV) operated at 10 mA emission current and 12 kV anode potential. XPS is sensitive to the composition of the first ten to twenty atomic layers, therefore is well suited to the direct detection of surface-segregated fluorocarbons in a hydrocarbon matrix. A wide (survey) scan and high resolution scans were carried out on each sample. High resolution scans were charge corrected to the main C 1s peak (285 eV) and then quantified to compare the amounts of each element present, using Kratos sensitivity factors.

Detection was carried out in FAT (fixed analyser transmission) mode, with pass energy of 80 eV for wide scans and pass energy 20 eV for high resolution scans. The magnetic immersion lens system allows the area of analysis to be defined by apertures, the 'slot' aperture of 300 × 700 μm was used for all wide/survey scans and high resolution scans. The take off angle for the photoelectron analyser is 90° and acceptance angle of 30° (in magnetic lens modes).

Scanning Probe Microscopy

Tapping mode AFM measurements were made using a Digital Instruments Nanoscope IV Multimode AFM equipped with a J-type scanner. Scans of 30 μm × 30 μm were carried out at 256 × 256 resolution in order to determine sample roughness. Height and phase maps were recorded using Arrow-NC-20 probes (Windsor Scientific, Slough, UK) with a nominal resonant frequency of ~300 kHz. Spin cast blended film samples were either studied directly in the instrument or annealed to 120°C then cooled to

room temperature prior to analysis. Optimal image quality was typically obtained with a scan rate of ~1 Hz and amplitude setpoint of 0.65 – 0.75 times the free space amplitude.

Ion Beam Analysis (^{3}He Nuclear Reaction Analysis)

Nuclear reaction analysis was used to make a direct determination of the depth distribution of the partially deuterated polyethylene additive in each blended film. Experiments were carried out at Durham University using a National Electrostatics Corporation (Middleton, Wisconsin) 5SDH Pelletron accelerator. A 2 mm diameter, 0.7 MeV beam of $^3He^+$ ions was directed to the sample surface at a grazing incidence of 7°. Following the D(3He, p)α reaction,[21] fast protons were detected at 170° to the incident beam. For these materials, data for two or more measurements of 3 μC $^3He^+$ ions taken on adjacent spots of the sample were summed in order to obtain good statistics with minimal corruption of the sample. The proton yield was corrected for the energy dependence of the nuclear reaction cross-section by division by the smoothed NRA spectrum of a perdeuterated polymer sample. The recoil energy was converted to a depth scale using the thick target approximation.[22] We have used this procedure reliably elsewhere for a variety of polymer systems.[23] Under these conditions the depth resolution at the surface is typically ~ 6 nm and due to straggling, depth resolution degrades at a rate of approximately 0.04 nm per nm of film traversed normal to the surface. The surface excess for polymer blend films, z*, is given by

$$z^* = h(\phi_s - \phi_b) \qquad (1)$$

where h is the thickness of the surface enriched layer, ϕ_s and ϕ_b are the surface and bulk concentrations respectively.

Neutron Reflectometry

Specular neutron reflectometry was carried out on the INTER reflectometer on the second target station of the STFC ISIS source, Rutherford Appleton Laboratories, U.K. Samples were placed on a temperature controlled stage and heated to 120 °C in order to ensure that the blended films were molten.

At this temperature, the bulk density of molten polyethylene with the same enchainment as our samples is 0.89 g/cm^3, which corresponds to a neutron scattering length density of 2.92×10^{-6} Å^{-2} and -3.2×10^{-7} Å^{-2} for the deuterated and hydrogenous polyethylenes respectively. Reflectivity was measured as a function of momentum transfer vector, Q ($=4\pi/\lambda \sin\theta$) from before the critical edge ($Q \sim 0.01$ Å^{-1}) to the point at which it became indistinguishable from background ($Q \sim 0.2$ Å^{-1}) using two angles of incidence, $\theta_{inc} = 0.6°$ and 1.8°. Data sets were recombined then scaled to R(Q)=1 in the critical range. Scaled data were multiplied by Q^4 to remove the Porod decay before fitting using a model concentration profile for the volume fraction of end functional polymer, ϕ, given by equation 2.

$$\phi(z) = \phi_\infty + \left(\frac{\phi_s - \phi_\infty}{2}\right)\left[1 + erf\left(\frac{h-z}{w}\right)\right] \qquad (2)$$

where w is the interfacial width of the adsorbed surface excess layer.

Results

Synthesis

The molecular weight data (obtained via GPC of the polybutadiene precursors) is summarized in table 1. Multi fluorocarbon end functionalized polyethylene additives were successfully prepared in a range of molecular weights with narrow polydispersity and sufficient deuterium labeling to enable characterization by ion beam and neutron scattering techniques. All of the materials were semi-crystalline at room temperature and analysis by differential scanning calorimetry at a heating rate of 10 °C/min gave melting transitions close to 100 °C. The structures of the functionalized polyethylenes are shown in figure 1. It is well established that the deuteration/saturation reaction of dienes with D_2 (catalysed by palladium) can also facilitate exchange of hydrogen isotopes between the gas and the polymer, so that deuteration results in a polymer containing, on average, more than two atoms of deuterium per saturated butadiene repeat unit.[19,24] Since the CF end functional groups and the moderate molecular weight of the functionalized polymer additives are likely to perturb the bulk density,

evaluation of the extent of deuteration is not possible by densimetry. Instead the H/D ratio was quantified by low energy elastic recoil detection[25] using Datafurnace software with evaluated scattering cross section data calculated by Gubrich.[26,27] The fraction of hydrogen atoms converted to deuterium, *f*, was in the range 0.38 +/- 0.05, which is consistently greater than the 0.25 that could be accounted for by addition across the double bonds alone. These values are consistent with those reported by Crist *et al*[19,28] for the saturation of polybutadienes by a similar method to make polyethylene homopolymers where exchange as well as saturation was observed.

Contact angle analysis

The influence of multi-end functional polyethylene additives on surface hydrophobicity is shown in figures 2-4 as a function of additive functionality (number of CF groups), additive molecular weight and homopolymer matrix molecular weight respectively. It can clearly be seen that all of the fluorocarbon end functionalized additives cause a marked increase the contact angle of water on the polymer blends, which steadily increases with increasing additive concentration. It is also evident that whilst the control additive, a low molecular weight deuterated polyethylene, dPE5 without any fluorocarbon groups (see figures 2 and 3) does appear to impart some increase in contact angle to matrix polymers, this effect is small compared with the corresponding fluorocarbon functionalized additives. From figure 4 it is apparent that there is very little influence of the matrix homopolymer molecular weight on contact angle.

In comparison to our results obtained previously for analogous amorphous polymer blends, there are two distinct differences that should be noted. Firstly the static contact angle data are significantly more scattered than is usually found for similar measurements on spin-cast films. Secondly the rate of increase of hydrophobicity is somewhat lower than we have previously observed for other polymers. Nevertheless, it is clear that within the experimental uncertainty, the additives do deliver a significant increase in blend surface hydrophobicity and in some cases reach literature values for PTFE (110°-115°).

Surface Properties

Tapping mode AFM height maps (figures 5(a)-(c)) show that 30 μm × 30 μm scans of polymer blend surfaces are typically rough on a scale of tens of nanometers. It is also important to consider the length scale on which these height variations occur, since this impacts upon the variation in surface gradient for a given root mean square (r.m.s.) roughness. In these films, variations in height are evident on a sub-micron scale, which although small, is still large compared to the vertical scale. Cross-sectional analysis of the blend surface reveals that the surfaces are rough, and that the surface topography regularly features gradients of up to 5° in magnitude.

We used AFM to explore the variation in surface topography as a function of sample cooling rate from the melt into the semi crystalline state. The height map in figure 5(a) corresponds to an unannealed sample, which has crystallized as the solvent evaporated during the spin casting process. Figure 5(b) shows the surface of an identical sample to the spin-cast film that was subsequently annealed above the melting temperature then allowed to cool slowly overnight in the vacuum oven. This resulted in crystallization occurring from a molten state (no solvent present) at a cooling rate of approximately 0.5 °C/min in the region of the melting point of the polyethylene components. In the other extreme, figure 5(c), the molten sample was removed directly from the annealing oven and plunged into liquid nitrogen. Whilst it is difficult to quantify the cooling rate of this procedure in the region of the melting transition, we believe that it is several orders of magnitude greater than the rate obtained by slowly cooling under vacuum. Subsequent analysis of the sample surfaces yielded values for the root mean square (r.m.s.) roughness of 8.4, 18.1 and 6.9 nm for the unannealed, slow cooled and rapidly cooled samples respectively.

We can derive from simple geometric arguments that an estimate of the 'typical' value of gradient, σ, of a surface that is wrinkled in two dimensions is given by

$$\sigma = \arccos\sqrt{\frac{A_p}{A_t}} \quad (3)$$

where, A_p is the projected area of the scan (=900 μm^2) with the measured surface area and A_t is the measured surface area. The measured surface areas for the unannealed, slowly cooled and rapidly cooled samples were 902, 903 and 901 μm^2 respectively, corresponding to σ values of 1.9, 2.7 and 3.3° respectively. This is consistent with our simpler analysis of the sample cross sections which showed that gradients of up to 5° were present, by typically the gradients were less than this value.

On a smaller scale, it is worth noting that AFM phase images, typified by figure 5(d), clearly reveal the crystalline nature of these films. The structure is quite reminiscent of the branched lamellar structures that have been reported for other thin spin cast semi crystalline polymer films.[29]

XPS results (figure 6) confirm that fluorocarbon is present in large quantities at the blended film surfaces. The percentage surface fluorocarbon was calculated from the elemental fluorine to carbon ratio, taking into account that 100 % C_8F_{17} fluorocarbon would comprise 68% fluorine and 32% carbon. Data for percentage fluorocarbon coverage are shown in figure 7 as a function of additive functionality, concentration and matrix molecular weight. It is clear from the XPS data that the surface fluorocarbon coverage increases systematically with increasing additive concentration. In general, the 2CFdPE5 blends have somewhat less surface fluorocarbon than their more fluorinated counterparts, and there appears to be relatively little difference in the amount of surface fluorocarbon between 3CFdPE5 and 4CFdPE5, consistent with our observations in analogous polystyrene films.[7] From a practical perspective it is important to establish the most efficient means to deliver fluorocarbon to the surface. A measure of this efficiency is to normalize the surface fluorocarbon content with respect to the bulk fluorocarbon content, (additive concentration × fraction of fluorocarbon per additive). When the data are represented in this way (figure 8) it becomes apparent that the 3CFdPE5 is the most efficient additive for achieving surface fluorination with the minimum possible amount of fluorine, with the

surface to bulk concentration ratio approaching 80. Although results are somewhat scattered, it appears that the efficiency of surface modification tends to decrease with increasing additive concentration.

Near surface properties

The surface enrichment of the fluorinated additives was further confirmed by nuclear reaction analysis experiments. Although these measurements have poorer surface sensitivity than XPS, and are sensitive to deuterium rather than fluorine, they have the advantage of simultaneously providing surface and near-surface concentration versus depth profiles of the additives. This additional information can be studied to explore the approach to equilibrium and reveal phase behavior. The influence of thermal history on identical samples is shown in figure 9. Apart from the unannealed data set, all of the samples were annealed for 1 hour at 120 °C – above the melting point after spin-coating. The annealed samples were then cooled to below the melting point of the film at a variety of rates. As was found in the AFM analysis, different cooling rates appeared to have a relatively modest effect on the measured behavior and the surface excess peak was similar in size for all of the annealed samples. Only the data for the unannealed sample was clearly distinct and in this case the surface excess peak was somewhat smaller than for the equivalent annealed samples. Figure 10 (a) and (b) show that whilst all the additives show a significant peak at the surface (depth ~ 0 nm), in some cases, notably with increasing additive molecular weight, there is also tendency to form an excess of additive at the substrate interface.

NRA data were fit using a simple three layer model convolved with instrumental resolution as we have established elsewhere for related amorphous systems.[30] The surface excess values obtained using equation 1 are shown in figures 11 (a-c) as a function of additive concentration and polymer structures. The NRA results were consistent with the XPS data in that there is a systematic increase in surface activity with increasing additive concentration in all cases. Surprisingly, however, there appeared to be no strong dependence of the surface excess on additive functionality, additive or matrix molecular weight. In our earlier work on amorphous polystyrene systems there was a strong dependence of

surface activity on additive functionality, with significant increases in hydrophobicity, lipophobicity and surface excess at low concentrations with increasing CF content per additive chain.[8] .

Whereas NRA is well suited to study semi-crystalline specimens at ambient temperatures, the converse case of molten samples is more easily addressed with neutron reflection. Figure 12 (a) shows specular NR data and fits for a series of 2CFdPE5 films at 120 °C. The data are shown as RQ^4 versus Q, to highlight the film structure. The Kiessig fringes corresponding to the total film thickness arise from interference between reflection at the film surface and the substrate interface and can be seen to grow in magnitude with increasing additive concentration.

The corresponding concentration profiles are shown in figure 12(b) which show that both the surface concentration and spatial extent of adsorbed additive increase with increasing concentration. The simultaneous measurement of the surface excess above and below the melting point can be compared in terms of the derived surface excess in figure 13. In the concentration region where the z^* values could be compared they appear to be very similar, indicating little influence of melting or crystallization on the near surface distribution of the additive polymers. For the molten polymers, the radius of gyration is given by[31]

$$R_g / nm = \left(kM_w / 6\right)^{1/2} \qquad (4)$$

where k is 0.0121 nm^2molg^{-1}, yielding an R_g value of 3.79 nm for the 2CFdPE5 additive. Using this relationship it is possible to calculate the surface excess for 2CFdPE5 as a function of blend composition and thermodynamic attraction of the chain ends to the air surface. The dotted line shows the SCFT predicted variation in surface excess for the 2CFdPE5 additive if the attraction of the functional groups to the surface, χ_b-χ_s is equal to 3.0 k_BT.[32-34]

Discussion

Materials

The results for the synthesis of multi-end functional polyethylene additives summarized in table 1, show that it is possible to create these materials with controlled molecular weight distribution and a

consistently high degree of end-capping. We should stress that this result could only be achieved with great care to ensure that the polymerization of butadiene was complete before addition of diphenylethylene, which was required in order to inhibit unwanted side reactions that otherwise results in reduced functionalization of chain ends. The final column of table 1 confirms the crystalline nature of the multi-end functional polyethylene additives, and the melting points approach the values found for the unfunctionalised matrix polymers. The difference in melting temperature is approximately 5-15 °C with the larger differences being found for the lower molecular weight additives. This observation suggests that the crystallinity is somewhat inhibited by the bulky fluorinated functional groups, and that this effect is most apparent when the functional group is bonded to a relatively small polyethylene chain. Notwithstanding these small differences in melting temperature, the materials are essentially highly similar to the bulk polymers that they were designed to modify, and in this respect are likely to be amenable to batch processing methods.

Surface modification

All of the synthesized polymers have a molecular weight which is well above the entanglement molecular weight of polyethylene[35] ($M_e \sim 1.15$ kg mol^{-1}); and therefore have the potential to form robust surface modifying layers that are entangled with the matrix subphase. The extent to which surface modification is achieved is most simply and clearly determined by contact angle measurements in which it can be seen that every multi-end functionalized additive causes a significant increase in hydrophobicity with increasing blend concentration, above that which can be achieved with the dPE5 control sample. In some cases, notably the higher concentrations of 3CFdPE5 and 4CFdPE5, the contact angle exceeds 110°, and is consistent with a smooth highly fluorinated (PTFE-like) surface characteristic.

The contact angle data in figure 3 suggest that within the experimental uncertainty, the molecular weight of the additive appears to have relatively little influence on surface hydrophobicity. This result is somewhat surprising since our earlier studies on amorphous systems all show that greater levels of

hydrophobicity are obtained with lower molecular weight additive when the functionality is constant. It is also noticeable that the increase in hydrophobicity is rather abrupt for every additive, and shows little concentration dependence after the initial increase at low concentrations. The extent of surface modification is also quite insensitive to the matrix molecular weight, figure 4. In this study, all of the matrix materials are higher in molecular weight than the additives; therefore we might expect that, if the behavior is similar to amorphous systems, the surface activity of the additives is independent of molecular weight.

In principle it is possible to extract surface energy measurements from the contact angle data with the use of multiple contact fluids. Further contact angle measurements were therefore attempted with dodecane and glycerol, with the intention of resolving the surface energy of the modified polyethylene films. However, it was observed that polyethylene films became slightly swollen by prolonged contact with dodecane, indicating that this was an inappropriate choice of contact fluid for accurate measurements. Since the polar and dispersive components of the surface energy of glycerol (γ_{disp} = 34 mJ m^{-2}, γ_{pol} = 30 mJ m^{-2}) are much less distinct than dodecane (γ_{disp} = 25.4 mJ m^{-2}, γ_{pol} = 0) is from water (γ_{disp} = 21.8 mJ m^{-2}, γ_{pol} = 51 mJ m^{-2}), the error in the surface energy calculation is very large without additional data from a nonpolar fluid that is not absorbed into the polyethylene.[16] Nevertheless, it was found that the fluorinated additives gave rise to increased contact angles from all three fluids (including dodecane contact angles of up to approximately 40°), indicating significant levels of surface fluorination had been achieved. This result has further significance since it demonstrates that not only is fluorocarbon present on the film surfaces, but it is also the case that the surface fluorocarbon does not either dissolve or rearrange itself within the polymer film to minimize contact with the dodecane on the timescale of the contact angle measurements. In other words, the fluorocarbon functionalized polyethylene additives do confer a robust form of surface modification to the blended films.

A more direct confirmation of surface fluorination was obtained from the XPS data which reveal that the surface fluorocarbon concentration far exceeds the bulk fluorocarbon concentration. As a measure of efficiency, this analysis shows that compared to PTFE, where fluorocarbon that fulfils a useful role at

the surface, but is also present at the same concentration where it is redundant throughout the bulk, these additives make very efficient use of fluorocarbon for the purpose of surface modification. In fact, we should stress that the XPS results for fluorocarbon content shown in figure 8 are likely to be a lower boundary to the true value for fluorocarbon content. This is because the C_8F_{17} fluorocarbon groups are approximately 1 nm in length, whereas the range probed by the XPS is of the order of 10 nm, albeit with greatest sensitivity to the composition of the first few atomic layers. Consequently even if the surface were 100% fluorocarbon, the molecular structure of the additives would ensure that some proportion of the surface region probed by XPS would also include hydrocarbon.

It is interesting to note that the increase in surface fluorocarbon with increasing bulk concentration is rather less abrupt than the changes in hydrophobicity would suggest. This indicates that the contact angle behavior is in fact a complex function of both chemical modification and topological modification by the presence of the additive. At low additive concentrations the additive may reduce the viscosity of the comparatively high molecular weight matrix, so enhancing the rate of crystallization and leading to an increase in roughness in the films. Conversely at higher additive concentrations, the surface behavior is dominated by the chemical contribution to surface hydrophobicity via the fluorocarbon groups.

Topology

One interesting possibility of these systems is that the combination of surface roughness and increased hydrophobicity could lead to superhydrophobic surfaces. This has been achieved by Lu et al, who successfully controlled the crystallization of polyethylene to create very rough surfaces.[36] Superhydrophobicity is typified by an absence of contact angle hysteresis and is often associated with very high (> 150°) contact angles. Although our contact angle measurements were static it was noted that samples could normally be tilted by several degrees without the droplets running off, which suggested significant levels of hysteresis. The hysteresis and modest increases in hydrophobicity are

consistent with Wenzel wetting rather the Cassie-Baxter wetting, and therefore with some increase in surface roughness it may yet be possible to obtain robust superhydrophobic surfaces.

The AFM height maps shown in figure 5 are typical of all of the samples analysed, irrespective of additive type, concentration or matrix, in that films were much rougher that would be expected for a corresponding amorphous spin-cast film.[8] The influence of the differing cooling protocols on surface topology is perhaps surprisingly modest, but it is nevertheless discernible that the spin-cast unannealed film (a) is composed of many small rough crystallites. When the same film is annealed then slowly cooled (b) both the height variation and the lateral scale of the features increases significantly, consistent with the formation of fewer larger crystal domains. Quenching the annealed sample rapidly (c) greatly reduces the vertical scale of individual features, but there is still a significant contribution to the r.m.s. roughness arising from the 'cracks' that appear on a lateral length scale of approximately 3-5 microns. The cracks are most likely to arise from the contraction of the blended films as they recrystallize from the melt, a process which is associated with a reduction in specific volume of ~10%, estimated from the difference in density between amorphous and linear low density polyethylene.[37]

Surface Segregation in Semi Crystalline Films

Nuclear reaction analysis results show the variation in additive volume fraction, ϕ, over a depth of ~100 nm. Although it is in principle possible to achieve marginally better depth resolution on smooth films over this range with grazing angles of incidence of less than 7° it was not found to improve the quality of data in these experiments. This is almost certainly due to the surface roughness that was apparent from the AFM measurements, which give rise to some variation in the true angle of incidence of the beam onto the sample surface. Nevertheless, the data in figure 9 show that the functionalized additive spontaneously migrates to the film surface, even during spin-casting to such an extent that a significant surface excess peak in concentration is visible at near zero depth. We have previously seen similar behavior for amorphous multi-end functional polymers. In this case however, annealing to just above the melting point of the blended films is sufficient to ensure rapid equilibration. This is evident

from the increase in magnitude of the surface excess peak and the absence of any depletion in concentration of the additive apparent in the region adjacent to the surface, which is a signature of diffusion limited surface segregation.[38] The self-diffusion of linear polyethylene prepared by saturation of polybutadiene was characterized by Crist et al in the 1980s.[19,28] Here it was established that the temperature dependence of self-diffusion, D^* follows

$$D^* \sim \frac{cT}{\exp\left(E_{D/T}/RT\right)} \qquad (5)$$

where $E_{D/T}$ is the diffusional activation energy (~23 kJ mol^{-1}), R is the gas constant, T is temperature and c is approximately 2.9x10^{-12} cm^{2}s^{-1}K^{-1} for 424 kg/mol PE. Further correcting for molecular weight dependence,[39] using D^* for entangled polymers scales with $M_w^{-2.3}$, we estimate diffusion coefficients for hPE50, hPE100 and hPE200 of 8.5 x10^{-11}, 1.7 x10^{-11} and 4.3 x10^{-12} cm^{2}s^{-1} at 110 °C respectively. The additive molecules, having much lower molecular weights would be expected to have higher diffusion coefficients still, although these values may be reduced somewhat by the presence of the functional groups, if these cause aggregation.[6,8] While we should treat these absolute values with considerable caution as the annealing temperature was only a few degrees above the melting temperature, we note that even the highest molecular weight matrix polymers are expected to diffuse by more than 1 μm in 1 hour of annealing. We should therefore be confident that the annealing process is sufficient to ensure that an equilibrium distribution is approached.

The different cooling regimes however seem to have relatively little effect on the magnitude of the surface excess peak, suggesting that the crystallization transition does not in this case cause significant levels of centre of mass movement for the different polymers. In these blends, this is most likely to be because the polymers are somewhat similar in composition and crystallization temperature, and it is quite probable that they undergo some degree of co-crystallization, albeit with the bulky CF groups excluded from the crystallites. Work is ongoing to elucidate the extent of miscibility of the additives and matrix polymers above and below the melting temperature but this is beyond the scope of this current paper.

The concentration profiles shown in figure 10 reveal that in addition to surface adsorption it is also possible in these thin films for the additive to accumulate to form significant excess quantities at the substrate. The substrate excess is less well resolved than the surface excess, partly due to ion straggling effects as the beam passes through the material, but partly also because of variations in film thickness and density due to roughness and crystallinity. Previously we have seen similar behavior in amorphous polymer systems under circumstances when the additive is incompatible with the matrix.[8] When this is the case there is no evidence for any fundamental attraction of the additive to the substrate interface but rather the formation of the excess at the air surface and the initial depletion of additive close to the surface leads to the oscillating concentration profiles commonly associated with surface directed spinodal decomposition.[40-42] Previously in multi-end functional polymer blends this behavior has only been seen when the functional group is large but the polymer chain of small. Here, however evidence for spinodal decomposition is also found when the polymer chain is comparatively large. This difference in behavior may indicate that in many cases the polyethylene chains themselves are not completely compatible. Deuterium labeling is known to give rise to a small positive Flory-Huggins interaction parameter, χ_{hd}, which was established by Nicholson[43] *et al* for similarly labeled PE homopolymers to be

$$\chi_{hd} = 1.14 \times 10^{-3} f^2 \qquad (6)$$

For the highest molecular weight combination of materials considered in this work, the geometric mean of the degree of polymerization of the components, N is approximately 1130, giving $\chi_{hd} N \sim 0.2$; therefore well below the threshold for phase separation at any composition. The fact that we do observe evidence for phase separation suggests that some other factors; the fluorinated end groups, and possibly also small variations in the 1,4 to 1,2 ratio in the microstructure between the additive and the matrix components contribute to an increased value for the effective Flory-Huggins interaction parameter.

The concentration dependence of the surface excess determined by NRA is noticeably different from many amorphous systems in that it has an almost linear dependence on concentration, as opposed to a sharp rise at low concentrations followed by a long plateau. Intriguingly, there appears to be little dependence of the surface excess on additive functionality, additive molecular weight or matrix molecular weight, even though both hydrophobicity and the fluorine content of the surfaces clearly increase with increasing fluorocarbon content of the additives. To some extent this apparent anomaly is mitigated by the fact that NRA is sensitive to deuterium and not fluorocarbon in the polymers. It therefore follows that for a given amount of deuterium found near the surface by NRA, the surface fluorocarbon content and hydrophobicity would still increase with increasing proportion of additive fluorination. When interfacial segregation of the additive occurs, as is evident in figure 10(b), it has the effect of reducing the amount of additive available in the interstitial region of the film that could migrate to the exposed film surface. We postulate that this effect is a limiting factor for the surface segregation of additive that would otherwise be very strongly adsorbed at the film surface, and that this is the main reason why the most highly functionalized (3CF and 4CF) dPEs do not have much larger z^* values than the corresponding 2CFdPEs. It is possible therefore that in thicker films where the substrate excess would have relatively little influence on the bulk concentration, significantly greater surface excesses would be found in the more highly fluorinated samples.

Surface Segregation in Molten Films

The neutron reflectometry data in figure 12 shows Kiessig fringes, which clearly increase in amplitude with increasing additive concentration. These fringes arise because of interference of the reflected neutron beam from the surface and the substrate interface of the film. In the absence of any adsorption at the film surface, there can be almost no reflection at the air surface because the scattering length densities of blended films are all very close to zero. It therefore follows that the Kiessig fringes provide a means to confirm and quantify the extent of 2CFdPE5 adsorption at the air surface of the molten blended films. Adsorption of the functionalised additives at the substrate interface would not

give rise to any fringes since this process would not contribute to reflection at the air surface of the film. The rate of damping of the Kiessig fringes with increasing Q is determined largely by the thickness of the surface excess layer. Therefore, when the amplitude of the reflectivity data is well fit over the entire Q range, we can be confident that the surface excess of the molten film is well characterized by the model. In our analysis of the NR data, the C_8F_{17} fluorocarbon groups were treated separately as they have a similar scattering length density to the partially deuterated polyethylene and comprise a small fraction of the additive polymer volume.

Results for the surface excess above and below the melting transition are compared in figure 13 and it is apparent that over a significant range of concentration they are broadly similar. Also included in figure 13 is an SCFT calculation of the surface excess from which is it possible to estimate the attraction of the functional groups to the film surface. Strictly, this analysis should not be applied to the semi crystalline state since there are significant density fluctuations within the polymer, however it is still valid to compare the data for this calculation with the surface excess values derived from neutron reflection in the molten state. The surface excess for the 2CFdPE5 additive is approximately consistent with the surface active groups having an affinity for the surface of approximately 3.0 k_BT. In our calculations we have neglected the interaction parameter between the polymer chains arising from isotopic labeling as χ_{hd} is of order 10^{-4} but we have taken into account the partial (84%) functionalisation of the additive polymer.

It is worth noting that this value is significantly lower than we have previously found for identically functionalized poly(lactide)[44] and poly(styrene)[8] materials, and is even slightly lower than the value obtained for a precursor polybutadiene material (ref Solomon paper) from which these additives were made. We should stress that this result underlines the fact that the attraction of the functional groups to the film surface is determined not only by the functional group, but also from the medium that surrounds it in the bulk. It is well known that fluorocarbon groups are less compatible with aromatic compounds than with aliphatic compounds, causing relatively strong surface adsorption at low surfactant concentrations in small molecule surfactant systems.[45] It is therefore not surprising that there

is less thermodynamic impetus to drive fluorocarbons to the surface of polyethylene polymer matrices than aromatic or polar matrices of polystyrene or polylactide.

Conclusion

We have demonstrated for the first time that polyethylene materials can be prepared having well-defined multiple fluorocarbon functional groups on chain ends with a high degree of reproducibility and with high efficiency of end-capping. These materials, when used as additives in blends can generate films with enhanced hydrophobicity and lipophobicity with surface properties approaching and in some cases exceeding those of PTFE. At room temperature the films have an appreciable degree of surface roughness when spin cast due to the inherent crystallinity of the materials. However, the roughness in these films was not sufficient to give rise to superhydrophobic surfaces, indicating that Wenzel rather than Cassie-Baxter wetting occurs. The roughness maybe controlled as a function of cooling rate from the molten state to the semi crystalline state. However, the self organization of the polymers within the films is not particularly sensitive to the cooling process since both the additives and the matrix polymer have similar crystallization temperatures.

Because these films are considerably rougher than their amorphous counterparts it is important to distinguish the influences of surface topology from surface chemistry on hydrophobicity. The presence of fluorocarbon groups at the surface of the films has been confirmed and quantified by XPS and shown to increase almost linearly with increasing additive concentration for many blends. Of the additives that we explored in this study, the most efficient additive for delivering fluorocarbon to the surface as a function of bulk fluorocarbon concentration was a relatively low molecular weight tri-functional polyethylene, 3CFdPE5, where the surface fluorocarbon concentration could exceed the bulk concentration by a factor of 80. Ion beam analysis revealed similar trends for the near surface distribution of the additives, however this measurement which is sensitive to the deuterated main chain of the additive rather than the fluorinated functional group did not display such a clear trend in order of surface activity between additives having different numbers of functional groups. Ion beam analysis

confirmed an absence of depletion adjacent to the surface, consistent with rapid equilibration when the samples are annealed above the melt temperature, and for higher molecular weight and more functionalized additives also showed an excess of additive at the film silicon interface, likely to be due to spinodal decomposition. The substrate excess, found for the more strongly incompatible (highly functionalized, higher molecular weight additives) may account for the relative lack of surface activity of these additives, since less of the material is available to migrate to the surface.

We compared the surface excess below the melting temperature measured by ion beam analysis with the corresponding value above the melt temperature by neutron reflectometry and found surface excess values to be very similar. Again this underlines our observation that the melting transition for these additives does not cause gross changes in their self organization. The thermodynamic adhesion of the functional groups to the surface is of order 3 k_BT which is significantly lower than for corresponding 2CF-PS (polystyrene) and 2CF-PLA (polylactide) blends reported in our earlier work. We should note however that the affinity of the fluorocarbon group for the film surface is measured in terms of difference in interaction between bulk and surface and that it is not surprising that different polymer matrices should give significantly different results for χ_s-χ_b for any given functional group.

ACKNOWLEDGMENT. We thank EPSRC for support of this work through EP/G032874/1, and the Nottingham Nanocentre and School of Chemistry, XPS laboratory for providing the XPS via EPSRC grant EP/F019750/1. We are also grateful to STFC (UK) for provision and support of the neutron facilities at ISIS. We thank Dr Alan Kenwright and Mr Doug Carswell for the expert support of the NMR and thermal analysis services.

Supporting Information Available. (1) Reaction scheme for the synthesis of multi-fluorocarbon end functional polyethylenes

FIGURE CAPTIONS

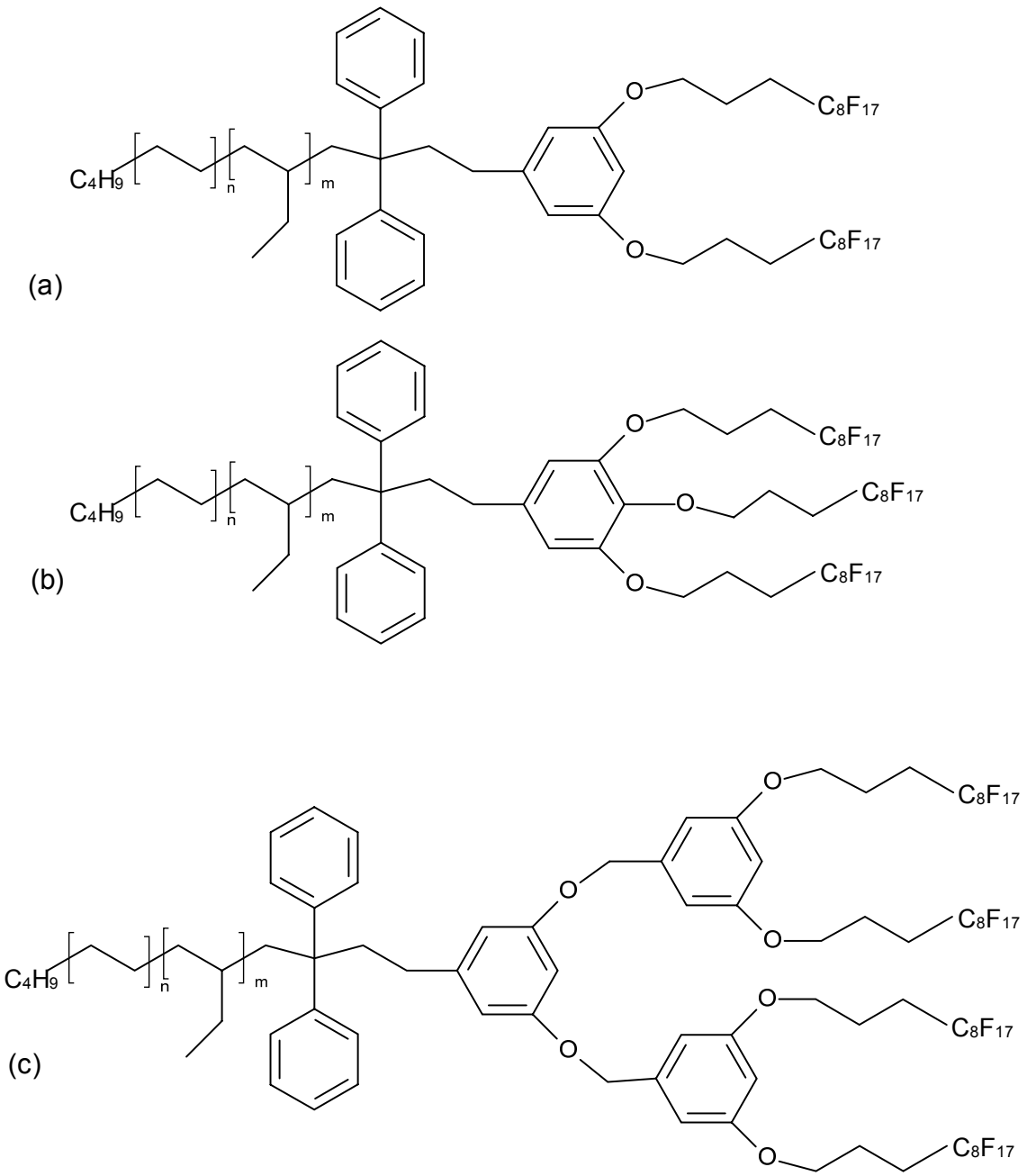

Figure 1. Sketch of molecular structures of multi-fluorocarbon end functionalized polymers; (a) 2CFdPE*y*, (b) 3CFdPE*y* and (c) 4CFdPE*y*, where y is the molecular weight of the polymer chain given by 0.058(m+n).

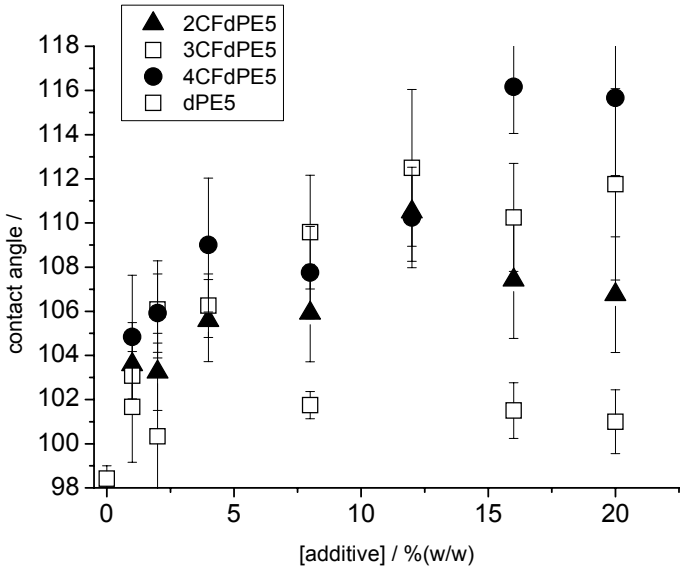

Figure 2. Water contact angle versus additive concentration for *x*CFdPE5 in PE200, where *x*=0 to 4, showing the influence of functionality on blend surface hydrophobicity.

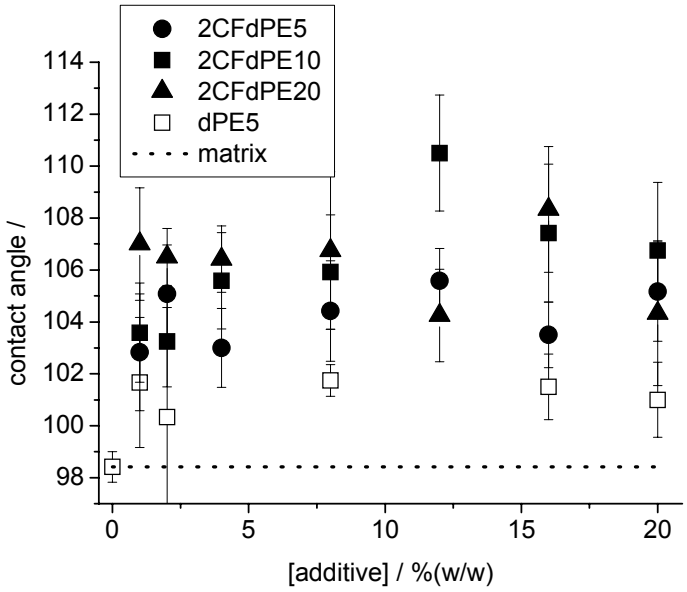

Figure 3. Water contact angle versus additive concentration for 2CFdPEy in PE200 matrix, showing the influence of additive molecular weight on blend surface hydrophobicity. The unfilled points correspond to an unfunctionalised control sample of 5 kg/mol. The dotted line indicates the contact angle measured on the matrix polymer without any additives.

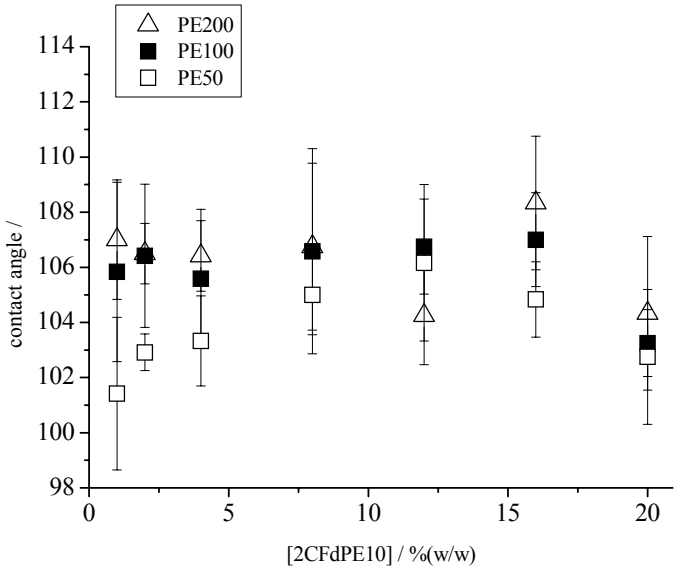

Figure 4. Water contact angle versus 2CFdPE10 concentration for different matrix molecular weights.

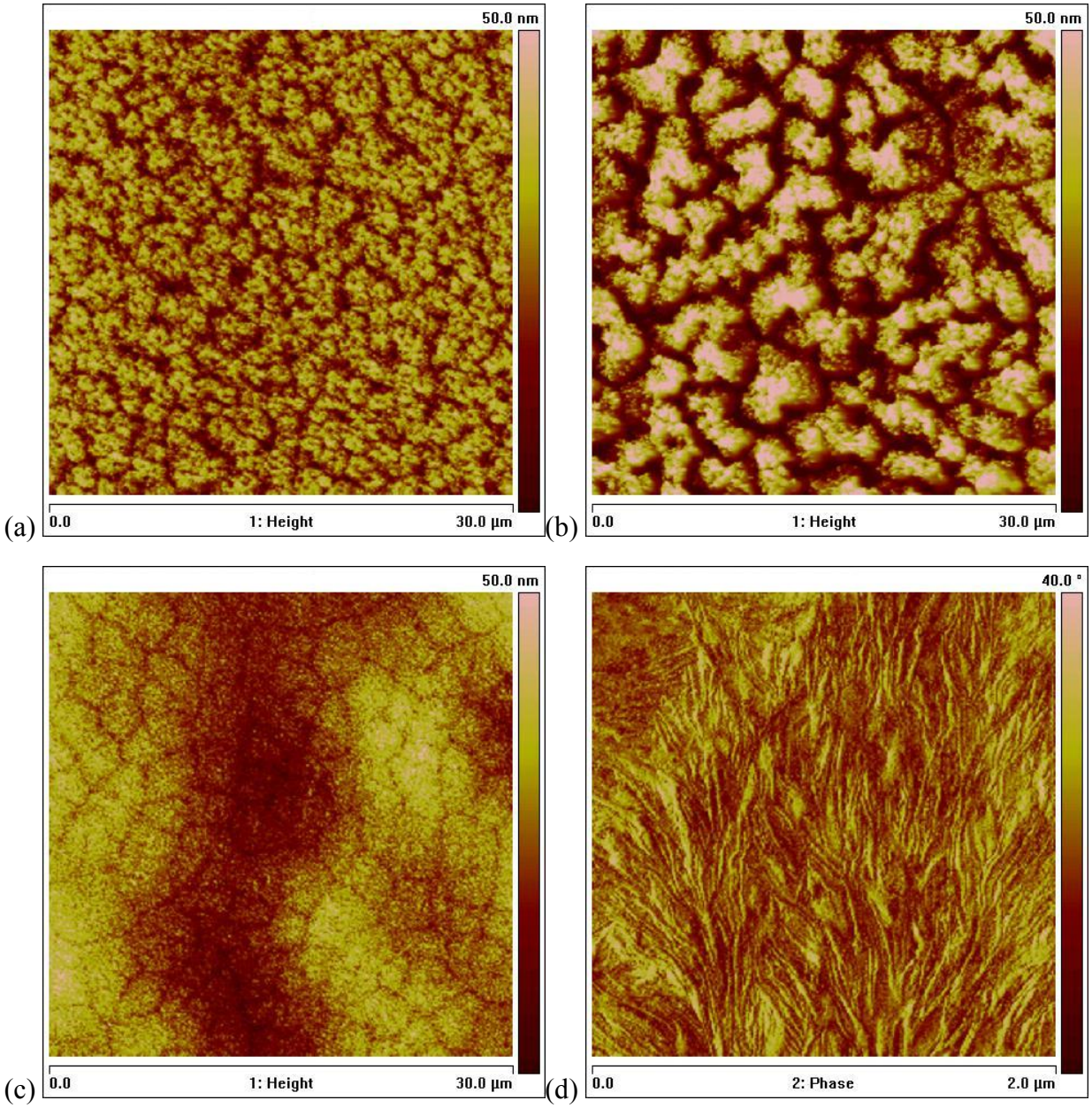

Figure 5. Tapping mode AFM height scans for 12% (w/w) 2CFdPE5 in PE100k, showing surface roughness as a function of cooling rate; height maps (a) spin-cast, not annealed, (b) annealed then cooled slowly in vacuum oven (c) annealed then cooled rapidly in liquid nitrogen. The semi-crystalline nature of the films is frequently apparent from the high resolution phase images (d).

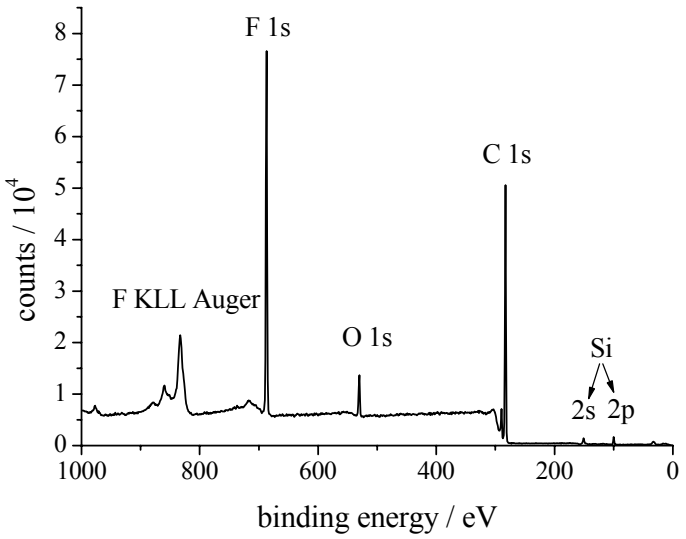

Figure 6. Typical XPS wide scan data for multi-fluorocarbon end functional polyethylene additives. Data shown are for 20% 3CFdPE5 in PE50k.

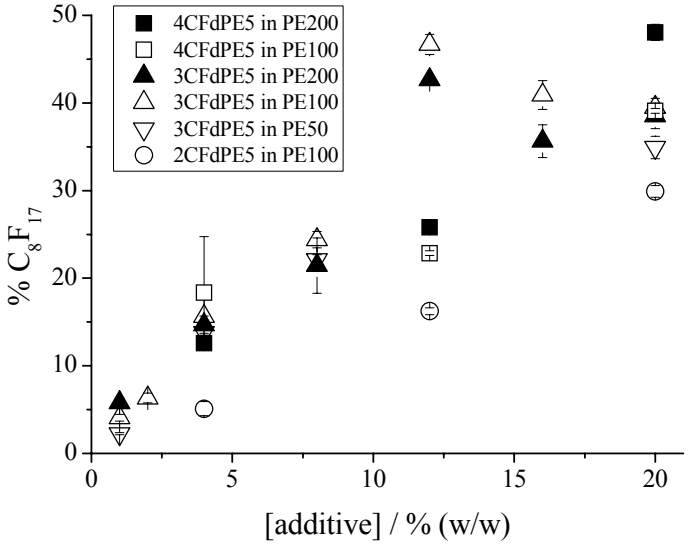

Figure 7. Fractional surface fluorocarbon composition derived from XPS data, showing influence of additive concentration on surface enrichment.

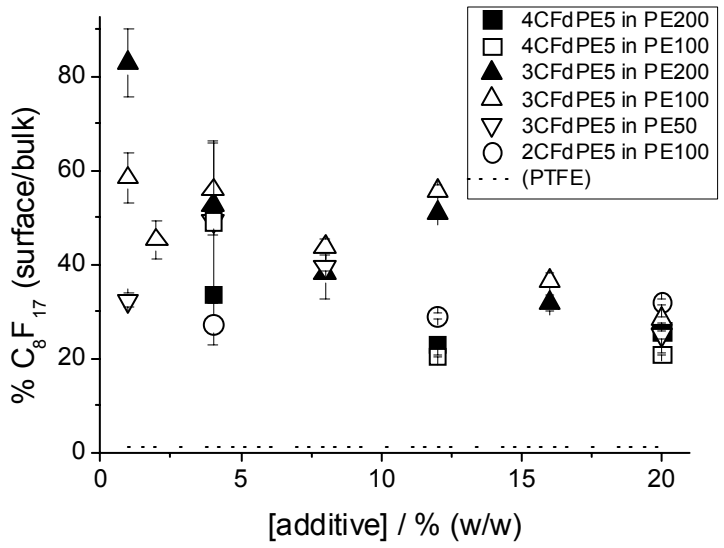

Figure 8. Adsorption efficiency (surface fluorocarbon/bulk fluorocarbon) versus composition and functionality for *x*CFdPE5 additives.

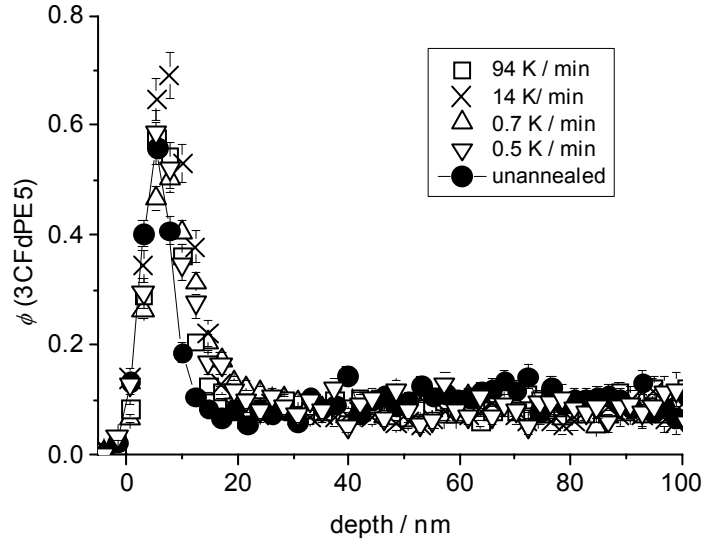

Figure 9. Normalised, reduced NRA data and fits for 12 % 3CFdPE5 in PE100 at different cooling rates.

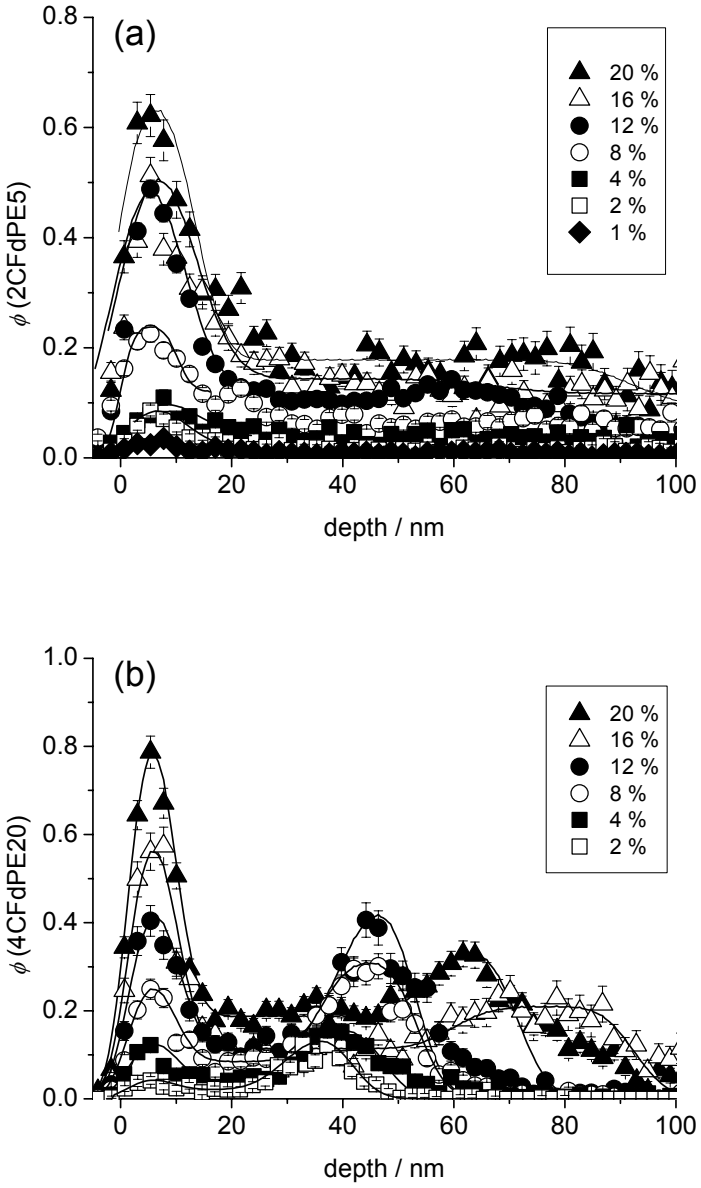

Figure 10. Normalized, reduced NRA data and fits for (a) 2CFdPE5 and (b) 4CFdPE20 in PE100.

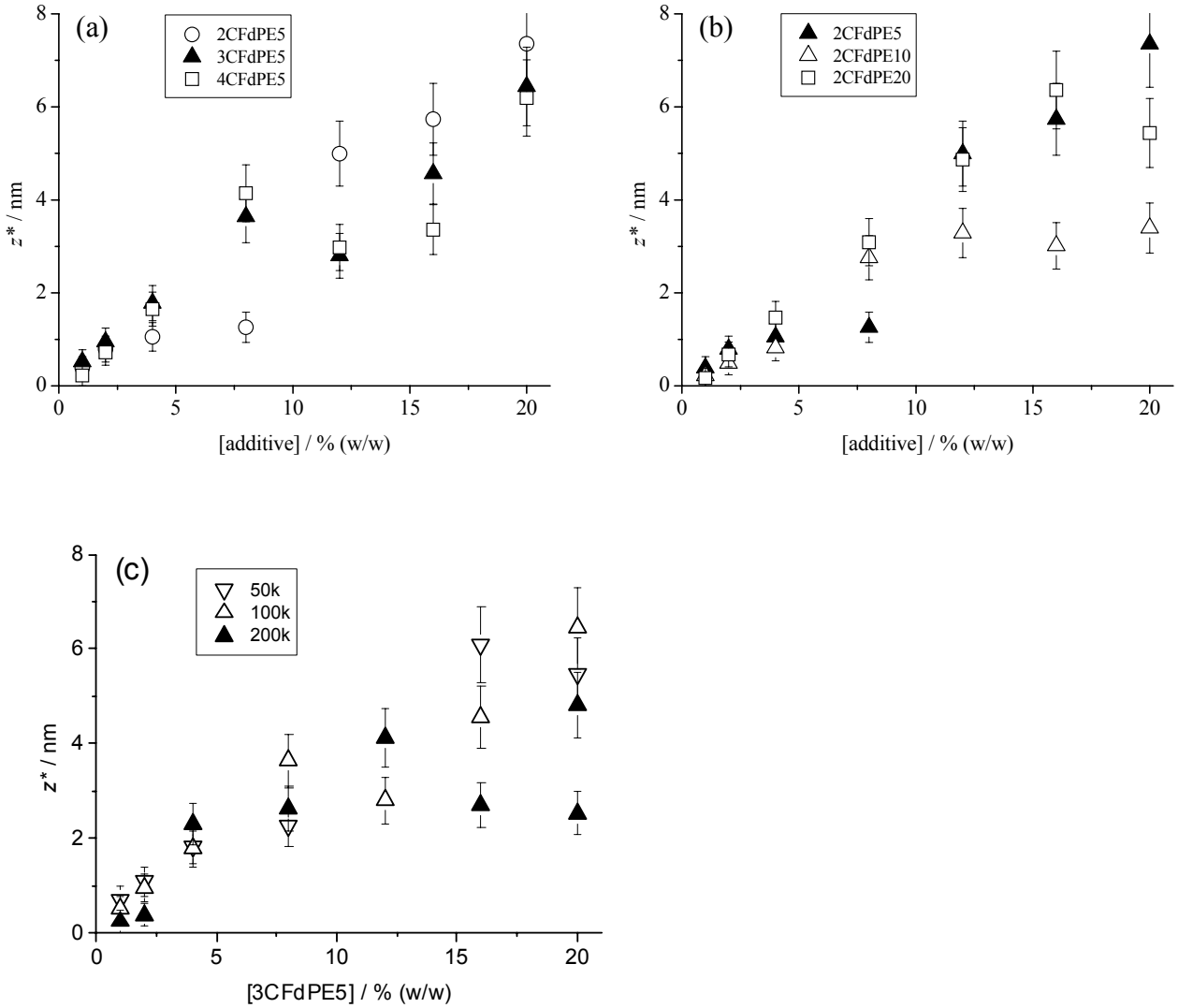

Figure 11. Surface excess derived from NRA experiments versus blend composition; dependence on (a) additive functionality in PE100 (b) additive molecular weight in PE100 (c) matrix molecular weight.

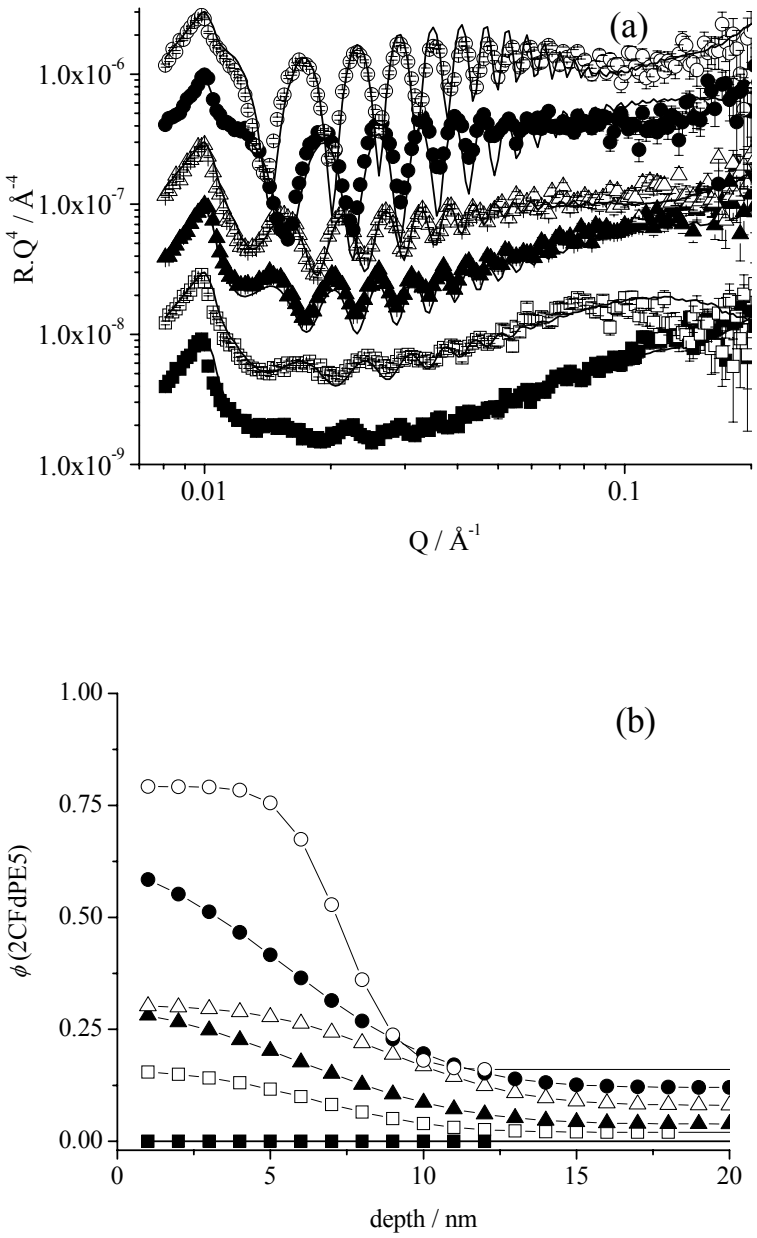

Figure 12. (a) Specular neutron reflectivity and fits versus concentration for 2CFdPE5 in PE50. Data shown are for 0% (solid squared) 2% (open squares) 4% (solid triangles) 8% (open triangles), 12% additive (solid circles) and 16% (open circles). Data and fits are shifted factors of $\sqrt{10}$ successively with increasing concentration for clarity. (b) Concentration profiles corresponding to the fits to NR data. The curves are fits to the data obtained using equation 1.

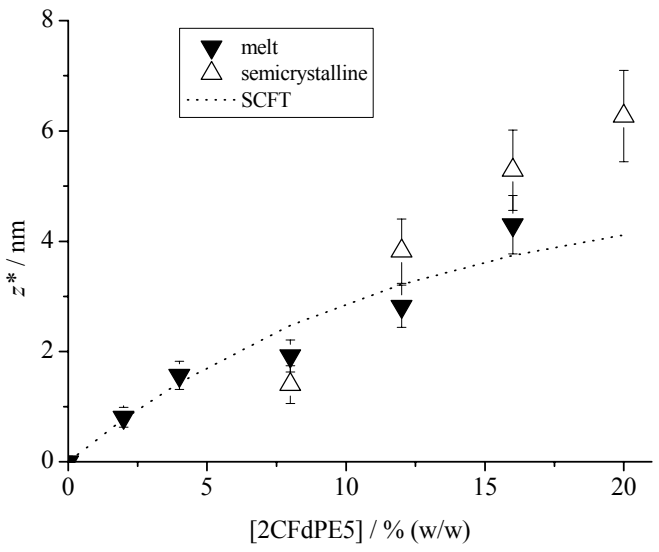

Figure 13. Comparison of surface excess derived above T_m by NR and below T_m by NRA for identical samples. The dotted curve indicates the SCFT predicted variation of surface excess for χ_b-χ_s = 3.0 k_BT.

Sample code	target M_n / kg mol^{-1}	measured M_n / kg mol^{-1}	M_w/M_n	% end-capping	f (=[D]/[H+D])	T_m / ºC
2CFdPE5	5	7.1	1.05	84	0.43	96
2CFdPE10	10	15.4	1.05	86	0.43	104
2CFdPE20	20	26.8	1.02	81	0.39	104
3CFdPE5	5	7.0	1.03	75	0.41	95
4CFdPE5	5	4.2	1.30	86	0.33	93
4CFdPE10	10	13.5	1.04	99	0.44	103
dPE5	5	4.9	1.02	-	0.35	104
PE50	50	56.6	1.04	-		106
PE100	100	113	1.04	-		110
PE200	200	205	1.02	-		109

Table 1. Summary of molecular weight data, percentage functionalization (end-capping), deuteration (f) and melting temperature (T_m) for polyethylene materials.

REFERENCES

(1) Chan, C. M.; Ko, T. M.; Hiraoka, H. *Surf. Sci. Rep.* **1996**, *24*, 3.

(2) Woodward, I.; Schofield, W. C. E.; Roucoules, V.; Badyal, J. P. S. *Langmuir* **2003**, *19*, 3432.

(3) Drabik, M.; Kousal, J.; Pihosh, Y.; Choukourov, A.; Biederman, H.; Slavinska, D.; Mackova, A.; Boldyreva, A.; Pesicka, J. *Vacuum* **2007**, *81*, 920.

(4) Schmidt, D. L.; Coburn, C. E.; Dekoven, B. M.; Potter, G. E.; Meyers, G. F.; Fischer, D. A. *Nature* **1994**, *368*, 39.

(5) Datla, V. M.; Shim, E.; Pourdeyhimi, B. *J. Appl. Polym. Sci.* **2011**, *121*, 1335.

(6) Hutchings, L. R.; Sarih, N. M.; Thompson, R. L. *Polymer Chemistry* **2011**, *2*, 851.

(7) Narrainen, A. P.; Hutchings, L. R.; Ansari, I.; Thompson, R. L.; Clarke, N. *Macromolecules* **2007**, *40*, 1969.

(8) Ansari, I. A.; Clarke, N.; Hutchings, L. R.; Pillay-Narrainen, A.; Terry, A. E.; Thompson, R. L.; Webster, J. R. P. *Langmuir* **2007**, *23*, 4405.

(9) Hirao, A.; Sugiyama, K.; Yokoyama, H. *Progress in Polymer Science* **2007**, *32*, 1393.

(10) Hardman, S. J.; Muhamad-Sarih, N.; Riggs, H. J.; Thompson, R. L.; Rigby, J.; Bergius, W. N. A.; Hutchings, L. R. *Macromolecules* **2011**, *44*, 6461.

(11) Thompson, R. L.; Narrainen, A. P.; Eggleston, S. M.; Ansari, I. A.; Hutchings, L. R.; Clarke, N. *J. Appl. Polym. Sci.* **2007**, *105*, 623.

(12) Walters, K. B.; Schwark, D. W.; Hirt, D. E. *Langmuir* **2003**, *19*, 5851.

(13) Koberstein, J. T. *Journal of Polymer Science Part B-Polymer Physics* **2004**, *42*, 2942.

(14) Norton, L. J.; Smigolova, V.; Pralle, M. U.; Hubenko, A.; Dai, K. H.; Kramer, E. J.; Hahn, S.; Berglund, C.; Dekoven, B. *Macromolecules* **1995**, *28*, 1999.

(15) Goffri, S.; Mueller, C.; Stingelin-Stutzmann, N.; Breiby, D. W.; Radano, C. P.; Andreasen, J. W.; Thompson, R.; Janssen, R. A. J.; Nielsen, M. M.; Smith, P.; Sirringhaus, H. *Nature Materials* **2006**, *5*, 950.

(16) Hardman, S. J. Ph.D. Thesis, Durham University, 2011.

(17) Kimani, S. M.; Hardman, S. J.; Hutchings, L. R.; Clarke, N.; Thompson, R. L. *Submitted to Soft Matter (RSC publishing, December 2011)* **2011**.

(18) Crist, B.; Graessley, W. W.; Wignall, G. D. *Polymer* **1982**, *23*, 1561.

(19) Bartels, C. R.; Crist, B.; Graessley, W. W. *Macromolecules* **1984**, *17*, 2702.

(20) Tanzer, J. D.; Crist, B. *Macromolecules* **1985**, *18*, 1291.

(21) Payne, R. S.; Clough, A. S.; Murphy, P.; Mills, P. J. *Nuclear Instruments & Methods in Physics Research Section B- Beam Interactions with Materials and Atoms* **1989**, *42*, 130.

(22) Composto, R. J.; Walters, R. M.; Genzer, J. *Materials Science and Engineering R* **2002**, *R38*, 107.

(23) Thompson, R. L.; McDonald, M. T.; Lenthall, J. T.; Hutchings, L. R. *Macromolecules* **2005**, *38*, 4339.

(24) Tanzer, J. D.; Bartels, C. R.; Crist, B.; Graessley, W. W. *Macromolecules* **1984**, *17*, 2708.

(25) Genzer, J.; Rothman, J. B.; Composto, R. J. *Nuclear Instruments & Methods in Physics Research Section B- Beam Interactions with Materials and Atoms* **1994**, *86*, 345.

(26) Barradas, N. P.; Jeynes, C.; Webb, R. P. *Applied Physics Letters* **1997**, *71*, 291.

(27) Gurbich, A. F. *Nuclear Instruments & Methods in Physics Research Section B-Beam Interactions with Materials and Atoms* **2010**, *268*, 1703.

(28) Crist, B.; Green, P. F.; Jones, R. A. L.; Kramer, E. J. *Macromolecules* **1989**, *22*, 2857.

(29) Wang, M. T.; Braun, H. G.; Meyer, E. *Macromolecules* **2004**, *37*, 437.

(30) Kiff, F. T.; Richards, R. W.; Thompson, R. L. *Langmuir* **2004**, *20*, 4465.

(31) Fetters, L. J.; Lohse, D. J.; Colby, R. H.; Mark, J. E., Ed.; American Institute of Physics: Woodbury, New York, 1996, p 335.
(32) Shull, K. R. *Macromolecules* **1996**, *29*, 2659.
(33) Jones, R. A. L.; Norton, L. J.; Shull, K. R.; Kramer, E. J.; Felcher, G. P.; Karim, A.; Fetters, L. J. *Macromolecules* **1992**, *25*, 2359.
(34) Shull, K. R. *Journal of Chemical Physics* **1991**, *94*, 5723.
(35) Fetters, L. J.; Lohse, D. J.; Milner, S. T.; Graessley, W. W. *Macromolecules* **1999**, *32*, 6847.
(36) Lu, X. Y.; Zhang, C. C.; Han, Y. C. *Macromol. Rapid Commun.* **2004**, *25*, 1606.
(37) Welsh, W. J.; Mark, J. E., Ed.; American Institute of Physics: Woodbury, New York, 1996, p 401.
(38) Thompson, R. L.; Hardman, S. J.; Hutchings, L. R.; Narrainen, A. P.; Dalgliesh, R. M. *Langmuir* **2009**, *25*, 3184.
(39) Lodge, T. P. *Physical Review Letters* **1999**, *83*, 3218.
(40) Geoghegan, M.; Jones, R. A. L.; Clough, A. S. *Journal of Chemical Physics* **1995**, *103*, 2719.
(41) Bruder, F.; Brenn, R. *Physical Review Letters* **1992**, *69*, 624.
(42) Jones, R. A. L.; Norton, L. J.; Kramer, E. J.; Bates, F. S.; Wiltzius, P. *Physical Review Letters* **1991**, *66*, 1326.
(43) Nicholson, J. C.; Crist, B. *Macromolecules* **1989**, *22*, 1704.
(44) Hutchings, L. R.; Narrainen, A. P.; Eggleston, S. M.; Clarke, N.; Thompson, R. L. *Polymer* **2006**, *47*, 8116.
(45) Binks, B. P.; Fletcher, P. D. I.; Sager, W. F. C.; Thompson, R. L. *Langmuir* **1995**, *11*, 977.

SYNOPSIS TOC

SUPPORTING INFORMATION

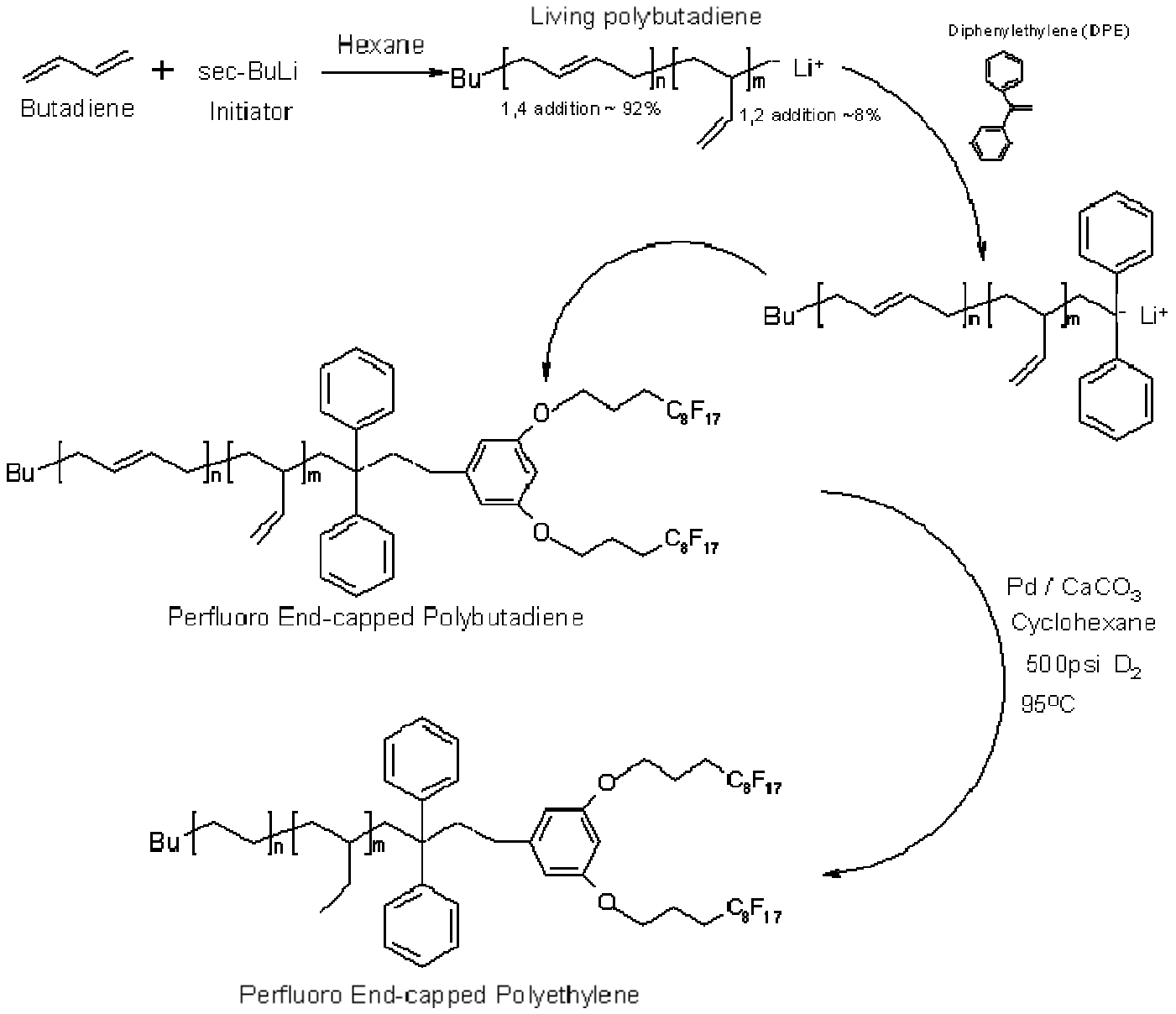

Scheme 1. Synthesis of Multi-Fluorocarbon End-Functional Polyethylenes.